Review

Structural Classification of Quasi-One-Dimensional Ternary Nitrides

David Andrew Headspith and Maria Grazia Francesconi *

School of Mathematics and Physical Science—Chemistry, and G.W. Gray Centre for Advanced Materials, University of Hull, Cottingham Road, Hull HU6 7RX, UK; dheadspith@hotmail.co.uk

* Correspondence: m.g.francesconi@hull.ac.uk; Tel.: +44-148-246-5409

Abstract: This review focuses on the crystal structural features of ternary (mixed-metal) quasi-one-dimensional nitrides i.e., nitrides containing (cation-N^{3-}) coordination polyhedra sharing either corners, edges, or faces, arranged in linear chains, and intercalated by a counter ion. The current relevance of these nitrides, and of quasi-one-dimensional compounds in general, lies in the fact that they are closely related to the pure one-dimensional systems (i.e., nanowires), which are vastly researched for their amazing properties closely related to their low dimensionality. A number of these properties were firstly discovered in quasi-one-dimensional compounds, highlighting the importance of expanding knowledge and research in this area. Furthermore, unlike oxides, nitrides and other non-oxide compounds are less developed, hence more difficult to categorise into structural classes that can then be related to other classes of compounds, leading to a fuller picture of structure–properties relationship. Within this context, this review aims to categorise and describe a number of ternary (mixed-metal) quasi-one-dimensional nitrides according to their structural features, specifically, the polyhedra forming the one-dimensional chains.

Keywords: nitrides; low-dimensional solids; mixed-metal compounds

1. Introduction

Traditionally, inorganic solid-state chemistry has focused on oxides. The chemistry of oxides has brought to attention a number of technologically exploitable phenomenon, such as high T_c superconductivity and colossal magnetoresistance [1–3]. The first example of a high-temperature superconductor (HTSC), $La_{1.8}Ba_{0.2}CuO_4$, found by Georg Bednorz and Alex Müller in 1986 [3], followed by $YBa_2Cu_3O_{7-x}$, the first compound to show superconductivity above the boiling point of liquid nitrogen and all HTSCs, which consist of copper oxide planes and show perovskite-like structures [4–6].

Research on non-oxide compounds has been slower in comparison, hence fewer examples are known. A significant factor in the slower development of non-oxide compounds (single and mixed-anion) has been the experimental challenge of synthesis and characterisation, as non-oxide materials need to be prepared in atmospheres different from air/oxygen and may, in some cases, be air/moisture-sensitive, necessitating air-free environments and additional experimental skills. The scarcity of non-oxide compounds, in comparison to their oxide counterparts, is an obstacle for understanding these solids, because we cannot describe, organise, and categorise structures geometrically to the extent we do with oxides, and we are therefore at a disadvantage in appreciating their physical properties. Consequentially, the discovery of new materials with potentially novel properties can be hindered.

The following review article aims to give an overview of quasi-one-dimensional ternary (mixed-metal) nitrides. The most widely known nitrides are binary nitrides—compounds formed

by one metal and the nitride anion, N^{3-}. These have been covered extensively in many papers and reviews, one of the most recent being published by R. S. Ningthoujam [7]. Simple binary nitrides have already offered up a number of interesting and useful properties to date. Many nitrides are exploited for their strength and hardness. Examples include AlN, HfN, and TiN, which can be used as scratch-resistant surfaces [8]. BN is commonly used as a refractory material, forming a lining in high-temperature devices, as a crucible material, or as an abrasive in the grinding of metals and alloys [8]. Simple binary nitrides like GaN and InN show extraordinary semiconducting properties. In fact, the 2014 Nobel Prize in physics was awarded to I. Akasaki, H. Amano, and S. Nakamura for their development of the GaN–AlN–InN family used for lighting technology; there is also a large and growing industry in power electronics based upon these binary nitrides [9]. The presence of another metal in ternary nitrides creates new and different materials and adds more flexibility for chemical tailoring, hence property/application targeting.

Quasi-one-dimensional and, in general, low-dimensional (1 and 2) solids are compounds with highly anisotropic bonds. Chains (quasi-one-dimensionality) or planes (quasi-two-dimensionality) of coordination polyhedra held together by strong ionic/covalent bonds are at a large distance from one another and held together by weaker bonds within the solid. Often, in ternary quasi-low-dimensional solids, the second metal lies within the separations between the chains/planes. This leads to electronic interactions between metals to be by far the strongest within the chains/planes, causing a high degree of anisotropy and unique properties [10]. For example, quasi-one-dimensional materials may show energetically discrete molecular states extending over large linear distances, and spin-charge separation predicted for a Luttinger liquid [11].

Nevertheless, interchain or plane interactions, albeit weak, cannot be completely discarded, hence the use of the prefix "quasi".

Pure one- and two-dimensional materials have come to have a great deal of attention more recently, particularly nanotubes or nanowires (one-dimensional systems) and nanosheets (two-dimensional sheets) [12–15]. Consequently, the long history of studies on quasi-low-dimensional systems is now becoming of enormous importance for understanding and comparing the properties of these new forms of materials.

In this review, following a brief summary of selected synthesis routes, a number of quasi-one-dimensional ternary (mixed-metal) nitrides is classified on the basis of coordination polyhedra forming one-dimensional chains within the crystal structure. It is the authors' hope that such a review will spark interest in these nitrides, with some of them to be considered as models or precursors for novel pure one-dimensional materials.

2. Synthesis Routes for Nitrides

A great deal of focus in solid-state chemistry has been placed on oxide materials because these compounds are easily prepared, generally in air or oxygen-rich atmospheres. Similar synthetic routes are not as successful when applied to nitrides. There are several reasons for this. In order to prepare nitrides from nitrogen gas, it is necessary to break the strong triple bond of N_2, a process that is thermodynamically unfavourable. In fact, the N_2 triple bond has a bond energy of 941 kJ·mol^{-1}, which is far stronger than the corresponding double bond of O_2 at 500 kJ·mol^{-1} [16]. The necessity to input large amounts of energy into breaking the triple bond increases the energies of formation of nitrides over oxides and results in a low standard free energy of formation. The high temperatures required to form the nitrides tend to favour decomposition due to the entropy gain in forming N_2 gas. The energy of formation of N^{3-} from N, 2300 kJ·mol^{-1}, is also particularly high when compared to other anions. The energy of formation of O^{2-} and S^{2-} is 700 and 331 kJ·mol^{-1}, respectively [16]. This reduces the effect of ionic bonding on the stability of nitrides. In fact, for ternary nitrides, it is common for a large amount of an electropositive metal to be required to stabilise the system via inductive effects. A further problem for many of the ternary nitrides is oxygen or moisture.

Decomposition to yield hydroxides/oxides and ammonia has meant that ternary nitrides often require inert atmospheres for handling and synthesis, which has slowed their development.

Despite difficulties in nitride preparation, there has been a great deal of progress in the synthetic approaches to nitrides in the last century. In the last few decades there have been a number of excellent reviews on nitrides and their synthesis [8,9,16–21]. Several of the more common preparative techniques are summarised here.

In spite of the difficulties in breaking the N≡N bond, it is still possible to synthesise a number of binary and ternary nitrides using nitrogen gas, at elevated temperatures, through traditional solid-state ceramic approaches. Ternary nitrides can be prepared by either the reaction of two metal powders under a nitrogen atmosphere or via reaction of metal nitrides with metals/metal nitrides [17]. Such approaches are simple, but limited by the number of metals which readily form binary (and higher) nitrides in nitrogen.

Lithium is the only alkali metal to readily form a nitride, Li_3N, from the reaction of lithium metal with nitrogen gas at 400 °C [18]. Li_3N can then react with other metals and/or metal nitrides to form ternary nitrides, as it can act as both the nitrogen source and reaction medium. In fact, Li_3N fluxes have been a common synthetic approach to lithium metal nitrides, as the low melting point of Li_3N (840–850 °C in N_2) facilitates intimate mixing of the reagents and favours crystal growth [17,22,23]. A vast majority of ternary nitrides contain lithium, due to their relatively simple synthesis. Juza et al. were the first group to investigate these lithium metal nitrides in 1940 [23].

Although the other alkali metals fail to react directly with nitrogen gas, their use in nitride synthesis has still been valuable. Sodium, for example, has found use as a solvent in nitride preparation [9]. Metals are dissolved/dispersed in the molten sodium and nitrogen gas absorbed into the mixture. By dissolving the metals, an increased surface area is generated, favouring a higher and more homogeneous diffusion of nitrogen into the solid. The nonreactivity of sodium towards nitrogen and its low boiling point are exploited, as the unreacted sodium can be removed by vacuum distillation or by washing with liquid ammonia to yield the metal nitride.

The preparation of alkaline-earth nitrides, from reactions with nitrogen gas and in sodium fluxes, have also proven effective, making up the second largest group of ternary nitrides [17,24].

However, nitrogen gas tends to favour the formation of subnitrides when reacting with certain metals, with only partial absorption of nitrogen, resulting in nonstoichiometric products [9,16]. For example, two alkaline-earth metals, strontium and barium, tend to produce the subnitrides Sr_2N and Ba_2N when reacted directly with N_2 gas [25,26]. These subnitrides exhibit interesting bonding, structural, and metallic properties. However, they present disadvantages when used as reagents to prepare ternary or more complex nitrides, via solid-state reaction, due to their low nitrogen stoichiometry. More reactive sources of nitrogen have been employed to prepare a range of nitrides in recent years.

One alternative to nitrogen is the solid nitrogen source sodium azide, which, when coupled with sodium fluxes, produce crystalline nitrides with sodium as a byproduct [9].

The most common alternative to nitrogen, however, is ammonia. This has been known to interact with metals for some time [27]. Firstly, ammoniation reactions take place at a lower temperature than reactions in nitrogen and can be performed on a wider range of starting materials, such as oxides, carbides, halides, and sulphides [9].

Organic molecules, such as urea and melamine, were also used as an ammonia/nitrogen source [28,29]. Heating pellets of ternary metal oxide and urea, for example, has resulted in M_3Mo_3N (M = Fe, Co) [28]. Unfortunately, these methods can result in samples of poor crystallinity or unwanted secondary compounds [9].

Nitrides may also be prepared via ammonolysis of metallorganic/complex precursors [19], for example, Fe_3Mo_3N, $FeWN_2$, Ni_2Mo_3N, Ni_3Mo_3N, and Ti_3AlN [30,31].

Another method, which has been used to synthesis ternary nitrides, containing two transition metals, is the reduction–nitridation of oxides under dilute hydrogen in nitrogen. This procedure can

be performed on ternary oxides, as in the synthesis of $Ni_{2-x}M'_xMo_3N$ (M' = Co, $0 \leq x \leq 1$; M' = Pd, $0 \leq x \leq 1.5$), $Fe_{2-x}M_xMo_3N$ (M = Ni, Pd, Pt), and $Fe_{3-x}Co_xMo_3N$ from binary oxides [32–35]. The advantage of this procedure is a relatively quick synthesis of high-purity phases from simple oxide precursors.

More complex methods have also been explored in order to improve the reactivity of nitrogen. These include plasma synthesis and high-pressure techniques. Plasma nitridation has been used to extend the use of dilute hydrogen in nitrogen to less reactive oxides. In this approach, metal oxides are reacted under a stream of microwave-induced H_2/N_2 plasma [36].

Through the use of high-temperature and high-pressure synthetic approaches, reagents that are unreactive under normal conditions can be forced together to give novel compounds. In addition, the application of pressure to known samples can induce structural transformation to yield new structural feature. Preparative methods range from simple autoclave synthesis to the use of more complex diamond anvil cells, which can apply up to 500 GPa of pressure [37]. This method is, however, limited by the availability of suitable equipment.

## 3. Crystal Structures of One-Dimensional Nitrides

The ternary nitrides, of interest in this review, contain an electropositive atom that stabilises the system via inductive effects. This electropositive element is usually an alkali, alkaline earth, or lanthanide metal. The second metal is commonly a transition metal, which has a tendency to form nitridometalate anions, MN_x^{n-} [38]. The coordination and connectivity of the nitridometalate anions dictates the main structural characteristics of the nitrides and influences the physical properties. In general, the early transition metals, in ternary nitrides, tend to favour relatively high oxidation states and high coordination numbers (4–6), while the late transition metals show lower oxidation states (0–2), and lower coordination [38].

Below are several of the better-known nitride systems, addressed in terms of their coordination of the metal nitrides. Although every effort has been made not to exclude any structurally significant compounds, some may have been unintentionally omitted.

3.1. Nitrides Containing Infinite Chains of Octahedra

In general, the ternary nitrides in which the transition metal (TM) shows high coordination numbers (5 or 6) with nitrogen tend to form rocksalt, perovskite, or layered structures and are commonly considered to contain TM–N polyhedra [38]. However, many subnitrides, containing a high metal-to-nitrogen ratio, contain chains of octahedra and are commonly described in terms of the nitrogen coordination. This will also be seen for the mixed-anion compounds in Section 3. The following are examples of ternary, s-block nitrides. $NaBa_3N$ ($P6_3/mmc$, $a = 8.4414(6)$ Å, $c = 6.9817(8)$ Å) and Na_5Ba_3N (*Pnma*, $a = 11.897(3)$ Å, $b = 7.056(2)$ Å, $c = 17.801(3)$ Å) are subnitrides showing six-cornered polyhedra with chains of Ba_3N [39–41]. $NaBa_3N$ consists of elongated face-sharing nitrogen-centred barium octahedra (trigonal antiprisms) running along [001]. These chains are hexagonally stacked and separated by sodium atoms at the centre of the triangular channels that the chains form, (Figure 1). As a result, the sodium atoms are coordinated to 12 barium atoms from the 3 nearest chains.

Na_5Ba_3N is very similar to $NaBa_3N$. Na_5Ba_3N has the same face-sharing Ba_6N octahedra. These chains show the same, if slightly distorted, hexagonal stacking arrangement, in this case running along [010]. The additional sodium increases the chain separation from 8.44 Å in $NaBa_3N$ to 10.70 Å in Na_5Ba_3N [40].
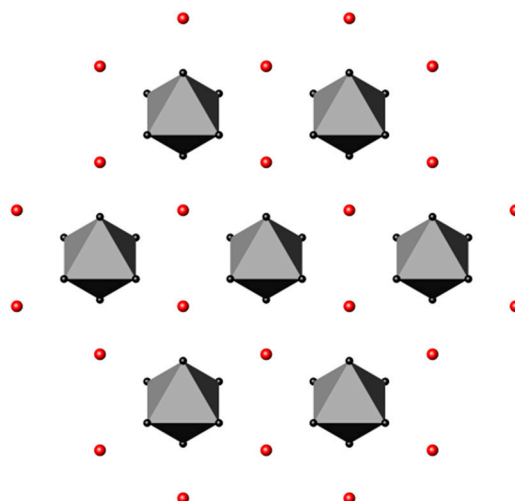
Figure 1. Representation of NaBa$_3$N viewed along [001]. The red and black spheres are sodium and barium, respectively. The grey polyhedra are Ba$_6$N.

3.2. Nitrides Containing Infinite Chains of Tetrahedra

Tetrahedral coordination of the metal in nitrides is particularly common. Compounds with a full range of structural features, from isolated tetrahedra to complex three-dimensional networks, are known to occur [38]. The following structures show chains of metal-centred nitrogen tetrahedra, showing either edge or corner connectivity.

The first-row transition metal lithium nitrides tend to fall into either of two structural groups: one based on superstructures of the fluorite structure and the other based on solid solutions of the Li$_3$N type [42]. In general, the transition metal elements adopting higher oxidation states have a preference for the fluorite-type structure, while the elements of lower oxidation state tend towards a Li$_3$N-related structure. The ratio between the cation sizes also plays a role, with anti-fluorite-related structures prevalent when the ratio is $r(\text{Li}^+)/r(\text{M}^{n+}) \geq 1$ [43]. Several of the transition metal compounds form structures in both these groups. In the Li–Fe–N system, solid solutions of the compositions Li$_{1-x}$Fe$_x$[Li$_2$N] $0 \leq x \leq 1$, Li$_{1-3x}$Fe$_x$[Li$_2$N] $0 \leq x \leq 1/3$, Fe$_{1.04}$[Li$_2$N]$_2$, and Fe[Li$_2$N]$_2$ show three-dimensional arrays based on Li$_3$N [42].

Li$_3$FeN$_2$, however, belongs to the anti-fluorite-like superstructural group of compounds with $r(\text{Li}^+)/r(\text{Fe}^{3+}) \approx 1.2$ [42,44,45].

The Li$_3$FeN$_2$ (*Ibam*, a = 4.872(1) Å, b = 9.641(3) Å, c = 4.792(1) Å) structure consists of a distorted cubic close-packed array of nitrogen atoms with the tetrahedral holes occupied by lithium and iron in a 3:1 ratio, respectively [42]. The FeN$_4$ tetrahedra are ordered in such a way as to result in chains of edge-sharing $^1_\infty$[FeN$_{4/2}^{3-}$] tetrahedra connected along [001]. These tetrahedral chains are in a similar arrangement to those found in SiS$_2$ [46]. In SiS$_2$, edge-sharing $^1_\infty$[SiS$_{4/2}$] units are hexagonally packed and held together by van der Waals interactions [46,47]. The chains in Li$_3$FeN$_2$ are also arranged with hexagonal rod-packing, but are separated by lithium-centred tetrahedra (Figure 2).
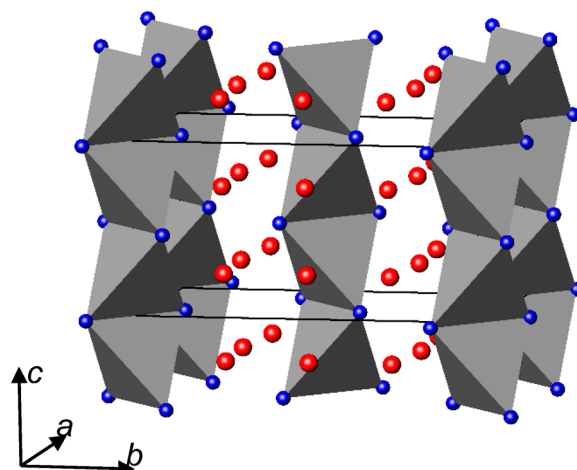
Figure 2. Representation of Li_3FeN_2. The red and blue spheres represent lithium and nitrogen, respectively. The chains of grey polyhedra represent the $\frac{1}{\infty}[FeN_{4/2}^{3-}]$ chains.

In this case, the nitrogen atoms are eight coordinate, surrounded by six lithium atoms and two iron atoms to give a distorted cube.

$A_3M_2N_4$ (A = Sr, Ba; M = Al, Ga), space group *Pnna*, also show SiS_2-like chains of tetrahedra [48–51]. In $A_3M_2N_4$, the nitrogen atoms are in a distorted-cubic close-packed arrangement, with a quarter of the tetrahedral holes occupied by Ga^{3+}/Al^{3+}, generating the $\frac{1}{\infty}[GaN_{4/2}^{3-}]/\frac{1}{\infty}[AlN_{4/2}^{3-}]$ chains in a similar way to Li_3FeN_2. Due in part to the larger size of Ba^{2+} and Sr^{2+} over Li^+, barium and strontium cations rest in three-quarters of the octahedral holes, rather than the smaller tetrahedral holes. The result is that the chains have a slight undulation of four tetrahedra, which run along [010] (Figure 3).
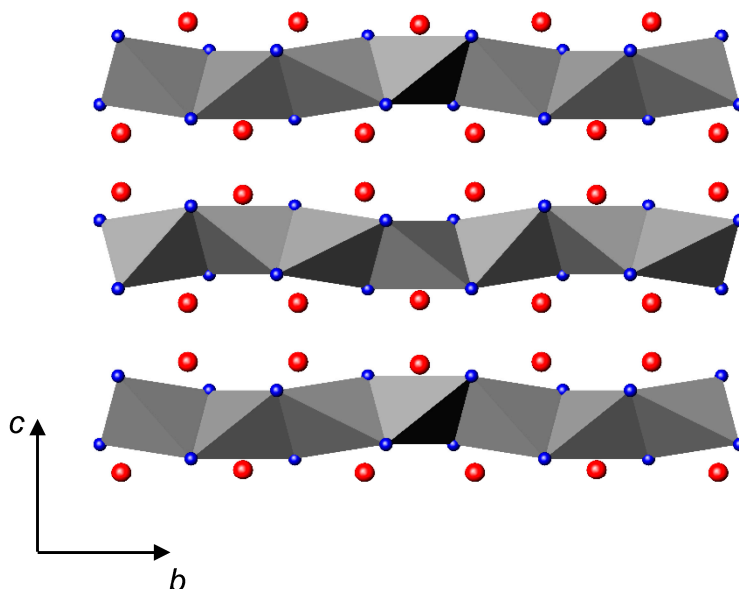
Figure 3. Representation of $Ba_3Ga_2N_4$. The red and blue spheres represent barium and nitrogen, respectively. The chains of grey polyhedra represent the $\frac{1}{\infty}[GaN_{4/2}^{3-}]$ chains.

Table 1 gives the unit cell parameters for $A_3M_2N_4$ (A = Sr, Ba; M = Al, Ga). As expected, the incorporation of a larger alkaline-earth cation into the structure results in increased unit cell dimensions.

Table 1. Unit cell parameters for $A_3M_2N_4$ (A = Sr, Ba; M = Al, Ga).

Compound	*a* (Å)	*b* (Å)	*c* (Å)
$Sr_3Al_2N_4$	5.901(3)	10.005(5)	9.580(4)
$Sr_2Ga_2N_4$	5.9552(6)	10.2753(8)	9.5595(9)
$Ba_2Al_2N_4$	6.179(2)	10.052(4)	10.230(4)
$Ba_2Ga_2N_4$	6.2010(12)	10.511(2)	10.070(2)

Another lithium compound showing an anti-fluorite-like structure with an $r(Li^+)/r(Ta^{5+}) \approx 1.2$ is $Li_4[TaN_3]$ (*Ibca*, $a = 4.9185(5)$ Å, $b = 9.7359(6)$ Å, $c = 14.150(1)$ Å) [44,45,52]. The nitrogen atoms form a distorted-cubic close-packed array, with lithium and tantalum occupying the tetrahedral holes in an ordered way. The TaN_4 tetrahedra are linked via the corners into $\frac{1}{\infty}[TaN_2N_{2/2}^{4-}]$ chains running along [100]. These chains have a repeating unit of two tetrahedra, giving a zigzaglike pattern along the chain. The site at the centre of the tetrahedron formed by the nitrogen atoms from three adjacent TaN_4 units remains vacant. The lithium occupies the remaining tetrahedral holes, surrounding the chains within an array of edge- and vertex-sharing LiN_4 tetrahedra. The result is a $1 \times 2 \times 3$ supercell with the Li_2O structure and the composition $Li_4\square[TaN_3]$ ($\square$ represents the cation vacancy). The Li–Ta–N system is not limited to the $Li_4[TaN_3]$ composition and structure; there is in fact a range of structures available, many of which do not show one-dimensional structures. $Li_7[TaN_4]$, for example, shows isolated $[TaN_4]^{7-}$ tetrahedra within a cubic close-packed array of nitrogen atoms, and $Li_{2-x}Ta_{2+x}N_4$ has a disordered rock-salt structure [52].

The following sodium metal nitrides all contain one-dimensional chains of tetrahedra, connected via shared vertices. Na_3WN_3 shows the *Cc* space group with $a = 13.810(8)$ Å, $b = 10.983(1)$ Å, $c = 6.395(1)$ Å, β = 117.48(3)° and Na_3MoN_3 also shows the *Cc* space group with $a = 13.854(5)$ Å, $b = 10.889(2)$ Å, $c = 6.366(2)$ Å, β = 117.23(3)° [53,54]. The MN_4 tetrahedra are corner-connected to give distorted $\frac{1}{\infty}[MN_2N_{2/2}^{3-}]$ chains. These chains run between the *a*- and *c*-axes in a sinusoidal manner, with a repeat unit of four tetrahedra (Figure 4).
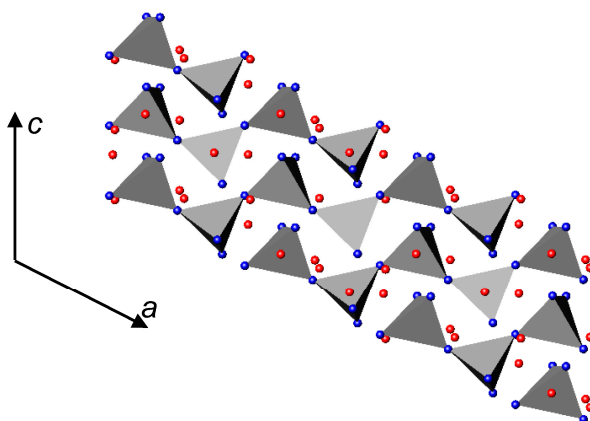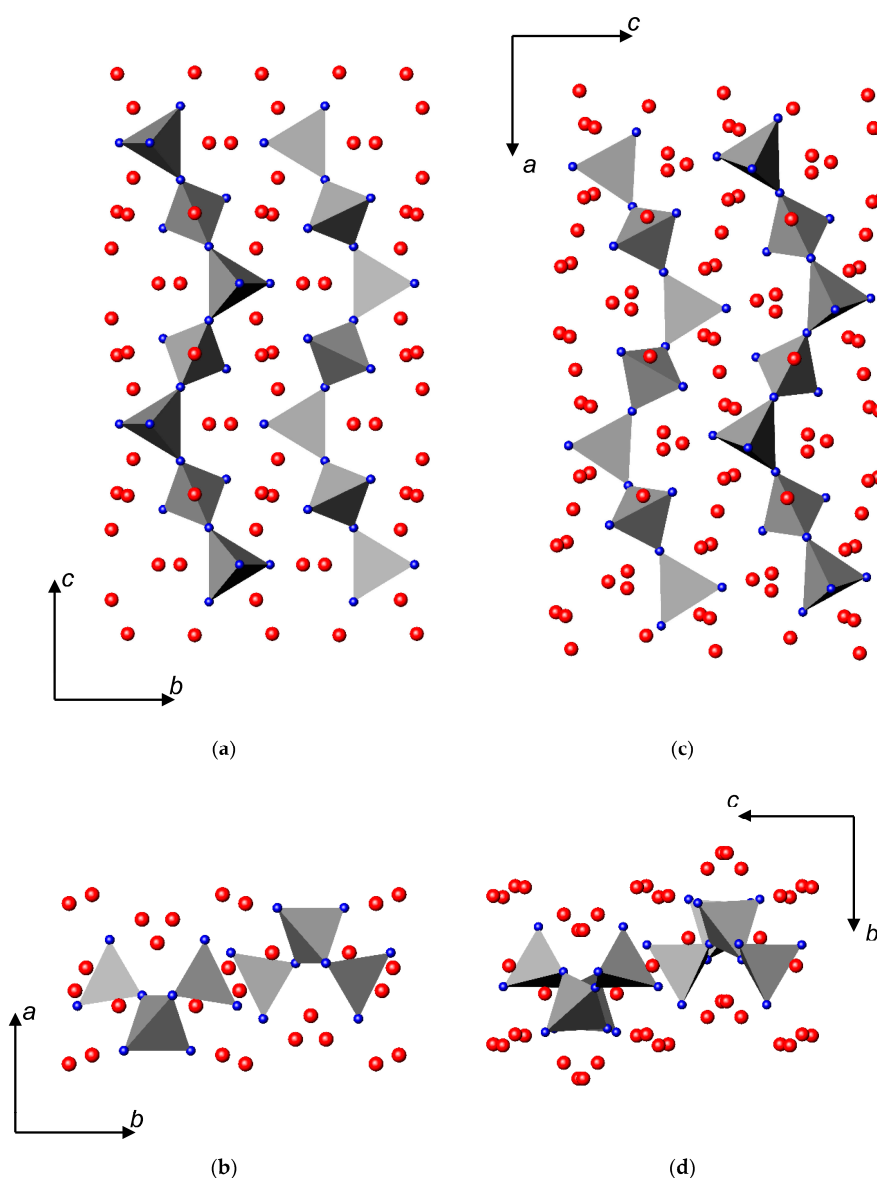

Figure 4. Representation of Na_3MN_3, M = W, Mo. The red and blue spheres represent sodium and nitrogen, respectively. The chains of grey polyhedra represent the $\frac{1}{\infty}[MN_{4/2}^{3-}]$ chains.

The chains show hexagonal rod-packing, with sodium sitting within the void between the chains [54].

The introduction of a larger electropositive metal onto the sodium site has the effect of altering the orientation of the WN_4 tetrahedra and, thus, the overall appearance of the chains. The other known alkali metal nitridotungstate (VI) compounds showing infinite chains are $Na_2K[WN_3]$, $Na_5Rb[(WN_3)_2]$, $Na_{11}Rb[(WN_3)_4]$, and $Na_5Cs[(WN_3)_2]$ [55,56]. The arrangement of tetrahedra in the chains of $Na_2K[WN_3]$ (*Pbcm*, $a = 6.3948(9)$ Å, $b = 11.924(3)$ Å, $c = 12.292(3)$ Å) and $Na_{11}Rb[(WN_3)_4]$

(*Pbca*, *a* = 11.701(3) Å, *b* = 12.140(3) Å, *c* = 12.502(2) Å) are quite similar, both being examples of unbranched vierer single-chain compounds (i.e., chains with a repeat unit of four tetrahedra). The chains in each compound are connected along the *c*- and *a*-axes respectively.

As stated above, a contributing factor to the structural variation is the larger size of the alkali metal cations. In $Na_2K[WN_3]$ there are two crystallographically independent potassium positions. The first potassium is coordinated to four nitrogen atoms in a distorted tetrahedral manner, in a similar way to $Na_3[WN_3]$, in which the sodium predominantly shows tetrahedral coordination. The second potassium rests in a larger hole, surrounded by 12 nitrogen atoms. It is this larger hole that is partially occupied by rubidium in the $Na_{11}Rb[(WN_3)_4]$ structure. The site is shared between rubidium and sodium in an ordered way, which is the cause of the increased unit cell volume when compared to $Na_3[WN_3]$. The WN_4 tetrahedra are then twisted around towards the sodium positions and away from the larger potassium and rubidium positions to give the winding chains shown in Figure 5 [55,56]. These broader chains show tetragonal rod-packing.

Figure 5. Representation of (**a**,**b**) $Na_2K[WN_3]$ and (**c**,**d**) $Na_{11}Rb[(WN_3)_4]$. The red and blue spheres represent sodium/rubidium and nitrogen, respectively. The grey polyhedra represent the $\frac{1}{\infty}[MN_{4/2}^{3-}]$ chains.

Increasing the rubidium content further gives $Na_5Rb[(WN_3)_2]$ ($P2_1/c$, a = 9.355(2) Å, b = 10.277(3) Å, c = 19.165(3) Å, β = 90.12(2)°) [55]. $Na_5Rb[(WN_3)_2]$ is isostructural to $Na_5Cs[(WN_3)_2]$ ($P2_1/c$, a = 9.403(3) Å, b = 10.236(2) Å, c = 19.501(4) Å, β = 90.01(2)°), and both show vierer chains, four repeating tetrahedra, of $^1_\infty[WN_2N_{2/2}^{3-}]$ running along [100] [55]. In these examples, the chains oscillate in the (010) plane with far less "twisting" when compared to Na_3WN_3 (Figure 6).
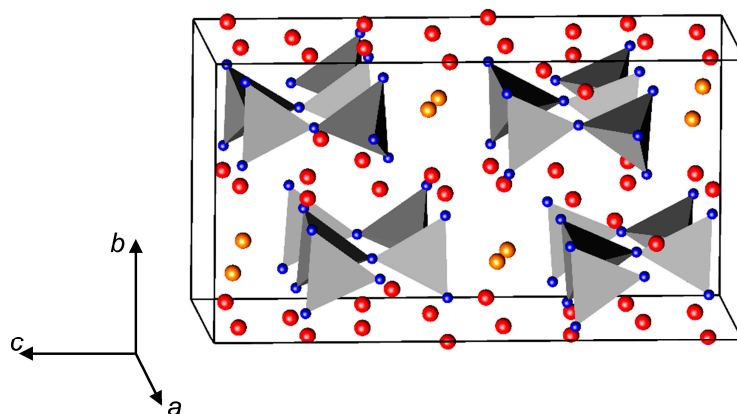
Figure 6. Representation of $Na_5Rb[(WN_3)_2]$. The red, orange, and blue spheres represent sodium, rubidium, and nitrogen, respectively. The grey polyhedra represent the $^1_\infty[MN_{4/2}^{3-}]$ chains.

The larger alkali metal (Rb or Cs) rests in distorted prismatic coordination, bound to nitrogen, forming layers parallel to the (010) plane. In compensation for the cation size, the chains are diverted around these sites. The sodium rests within the loops of the chains, and also to the sides, separating them along [010]. Hence, the sodium remains either in an approximately tetrahedral coordination. This can be extended to include an additional atom, described as 4 + 1 coordination.

The family of A_2MN_3 nitrides (A = Sr, Ba; M = V, Nb, Ta) all show chains of edge-sharing MN_4 tetrahedra. The unit cell parameters are given in Table 2. A_2MN_3 (A = Sr, Ba; M = Nb, Ta), Sr_2VN_3, and Ca_2VN_3 are isostructural with Ba_2ZnO_3 [57,58]. These are examples of zweier single-chain compounds (i.e., containing a repeat unit of two tetrahedra). These chains run parallel to [100]. The Ba^{2+}, Sr^{2+}, and Ca^{2+} cations lie on two crystallographically independent sites, both seven coordinate, A(1) is in distorted pentagonal bipyramidal coordination and A(2) shows monocapped trigonal prismatic coordination [59].

Table 2. Selected structural properties of A_2MN_3 (A = Sr, Ba; M = V, Nb, Ta) and Ca_2VN_3 [57–59].

Compound	Space Group	a (Å)	b (Å)	c (Å)	β (°)
Ca_2VN_3	$C2/c$	5.59538(5)	10.41027(1)	11.62243(1)	92.342(1)
Sr_2VN_3	$C2/c$	5.71036(9)	10.9521(2)	12.2881(2)	90.986(1)
Sr_2NbN_3	$C2/c$	5.9864(2)	11.2271(3)	12.5465(4)	92.587(2)
Sr_2TaN_3	$C2/c$	5.9832(2)	11.2832(2)	12.5814(2)	92.26(1)
Ba_2VN_3	$Cmca$	5.8614(4)	11.4682(7)	12.9121(9)	90
Ba_2NbN_3	$C2/c$	6.132(3)	11.768(3)	13.229(4)	91.65(2)
Ba_2TaN_3	$C2/c$	6.130(3)	11.815(4)	13.263(5)	91.2(1)

Increasing the size of the A cation results in straighter chains, and therefore, a reduction in the monoclinic distortion, similar to the Na–Rb–Cs–W–N systems mentioned previously.

3.3. Nitrides Containing Infinite Chains of Square Planar Units

Ternary nitrides containing transition metal centres in low oxidation states show some unusual coordination. A_2MN_3 (A = Th, U, Ce; M = Cr, Mn) contain M^+ cation, which form one-dimensional chains of planar MN_4 [60–64].

A$_2$MN$_3$ (A = Th, U, Ce; M = Cr, Mn) are isostructural to Sr$_2$CuO$_3$ showing an orthorhombic anion deficient T-type structure. In 1970, Benz et al. reported the crystal structure of A$_2$MN$_3$ (A = Th, U; M = Cr, Mn) with space group *Immm* (unit cell parameters are given in Table 3), as consisting of corner-linked chains of MN$_4$, which are in approximately square-planar geometry [60]. These $^1_\infty[MN_2N^{8-}_{2/2}]$ chains are linked along the *a*-axis and show hexagonal rod-packing. The square planar units are all orientated to lie parallel to the (010) plane, and each MN$_4$ unit sits within a cuboid of A^{4+} cations. The nitrogen atoms show two crystallographically independent positions and a near octahedral coordination. N(1) bridges two transition metal centres and is surrounded by four A atoms, while N(2) is the terminal nitrogen position and, therefore, is bound to a single transition metal and five A atoms. Each A is located roughly at the centre of a monocapped trigonal prism of nitrogen anions.

Table 3. Unit cell parameters for A$_2$MN$_3$ (A = Th, U, Ce; M = Cr, Mn) [60–64].

Compound	*a* (Å)	*b* (Å)	*c* (Å)
Th$_2$CrN$_3$	3.8654(5)	3.5154(2)	12.8446(19)
U$_2$CrN$_3$	3.7397(3)	3.3082(3)	12.3335(7)
Ce$_2$CrN$_3$	3.7900(10)	3.4040(10)	12.5170(2)
Th$_2$MnN$_3$	3.7919(3)	3.5482(2)	12.8321(4)
U$_2$MnN$_3$	3.7216(6)	3.3274(2)	12.2137(8)
Ce$_2$MnN$_3$	3.74994(6)	3.44450(6)	12.4601(2)

The structure may also be thought of as an anion-deficient K$_2$NiF$_4$-type structure. K$_2$NiF$_4$ is an *n* = 1 Ruddlesden–Popper, A$_{n+1}$TM$_n$O$_{3n+1}$, compound. K$_2$NiF$_4$ consists of two-dimensional layers of corner-sharing NiF$_6$ octahedra. Each octahedron is surrounded by eight K$^+$ cations in an analogous way to the perovskite structure. These perovskite layers are interleaved by a NaCl-type spacer unit of alkali metal and fluoride ions. Removal of half the equatorial anions in an ordered way generates the MN$_4$ chains seen in A$_2$MN$_3$.
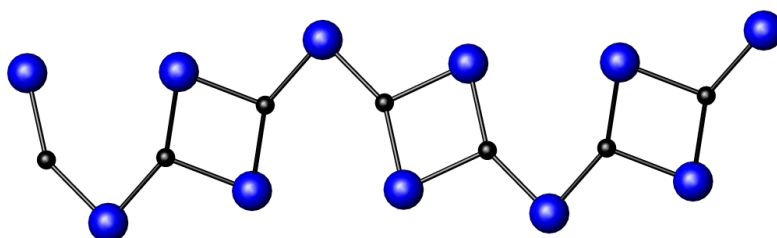
3.4. Nitrides Containing Infinite Chains of Triangular Units

LiCaN (*Pnma*, *a* = 8.471(3) Å, *b* = 3.676(2) Å, *c* = 5.537(3) Å) is another example of a lithium compound adopting the anti-fluorite-type structure [21,43]. In this case, calcium occupies half the tetrahedral holes and lithium occupies the other half, distorted from the centre. These are ordered in such a way as to give planes of edge-sharing LiN$_3$ triangular units, as shown in Figure 7.
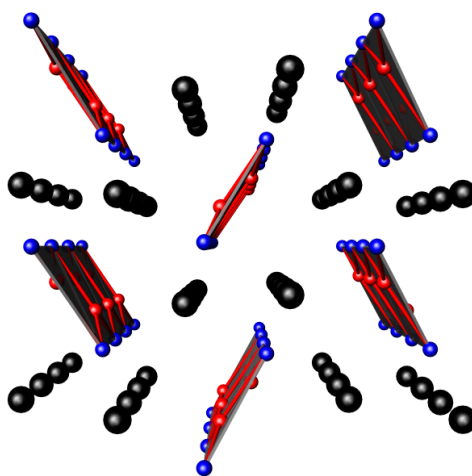
Figure 7. Representation of LiCaN, viewed along [010]. The red, blue and black spheres indicate lithium, nitrogen, and calcium, respectively.

Alternatively, compounds can also show transition metal-centred triangular units. $Sr_2Li[Fe_2N_3]$ ($C2/c$, a = 6.559(1) Å, b = 11.414(2) Å, c = 6.593(1) Å) and $Ba_2Li[Fe_2N_3]$ ($C2/c$, a = 6.875(2) Å, b = 11.781(4) Å, c = 6.809(2) Å) contain $[(FeN_{3/2})_2^{5-}]$ chains, as shown in Figure 8 [65]. Each iron is in distorted trigonal-planar coordination to nitrogen. These FeN_3 units are linked via two shared nitrogen atoms. The $[(FeN_{3/2})_2^{5-}]$ units are then linked via the remaining nitrogen. The chains are separated along [101] by lithium atoms forming $\frac{1}{\infty}\{Li_{2/2}\,[(FeN_{3/2})_2^{4-}]\}$ layers. These layers are surrounded by the strontium/barium atoms in distorted trigonal-bipyramidal coordination to nitrogen.


Figure 8. Representation of the $[(FeN_{3/2})_2^{5-}]$ chains of $Sr_2Li[Fe_2N_3]$. The blue and black spheres are nitrogen and iron, respectively.

3.5. Nitrides Containing Infinite Linear Chains

Coordination two, of the transition metal, is a less common coordination in ternary nitrides. Linear coordination occurs for several of the late transition metals in low oxidation states, +1 and +2 [66]. Those nitrides with transition metals in +1 oxidation state tend to form infinite linear metal nitride chains. These chains can take several orientations: straight, zigzagged, or helical.

Cationic substitution of the lithium in LiCaN can yield $Ca[(Ni_{1-x}Li_x)N]$ ($0 \leq x \leq 0.58$). This solid solution has a different structure from the parent compound, with $\frac{1}{\infty}[Ni_{1-x}Li_xN_{2/2}^{2-}]$ linear chains, and the CaNiN-type structure [67].

CaNiN ($P4_2/mmc$, a = 3.5809(2) Å, c = 7.0096(3) Å) was discovered in 1990 by DiSalvo and found to contain $\frac{1}{\infty}[NiN_{2/2}^{2-}]$ linear chains [68]. These form planes of parallel chains, which are stacked along the c-axis. The chains alternate between running along [100] and [010] moving along [001] (Figure 9). The calcium sits in tetrahedral coordination with four nitrogen atoms.
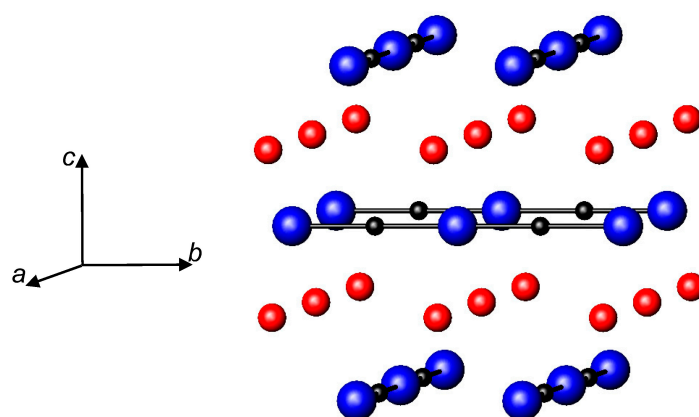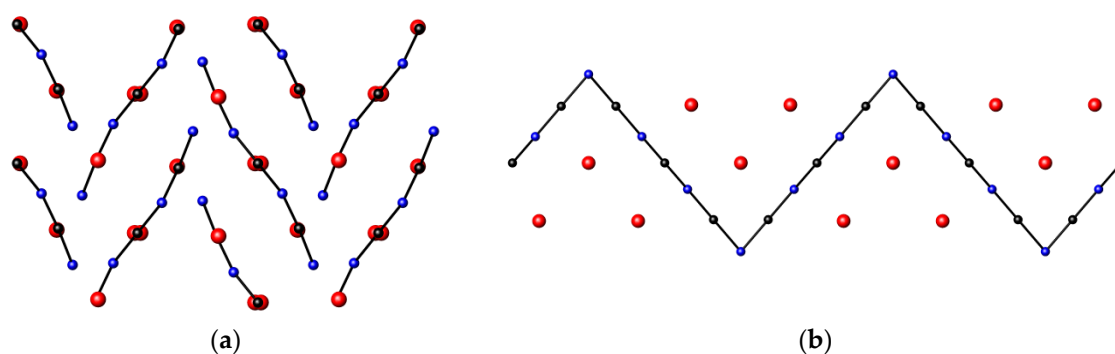

Figure 9. Representation of CaNiN. The red, black, and blue spheres represent calcium, nickel, and nitrogen, respectively.

Introduction of strontium onto the calcium site, $Ca_{1-x}Sr_xNiN_3$, up to $x \approx 0.5$ acts to increase the unit cell dimensions of CaNiN, but the overall structure remains the same [69,70]. The increase in unit cell dimensions is more significant in the c-axis, as it is easier for the structure to accommodate the

larger cations by increasing the perpendicular interchain separation along *c*, while the criss-crossing of the chains along *a* and *b* restricts expansion due to the limiting Ni–N bond distances.

The LiSrN ($I4_2/mmc$, *a* = 3.924(3) Å, *c* = 7.085(4) Å), unlike LiCaN, also adopts the CaNiN structure [71]. Substitution of the lithium cation with nickel gives $SrLi_xNi_{1-x}N$ ($0 \leq x \leq 0.52$) and induces a structural transformation [21]. The transformation is to the SrNiN structure (*Pnma*, *a* = 9.0859(4) Å, *b* = 13.230(93) Å, *c* = 5.2473(3) Å), which contains zigzagging $\frac{1}{\infty}[NiN_{2/2}^{2-}]$ chains [70]. The chains run along [010] and alternate directions by 78° on every third nitrogen down the chain, producing the zigzag. The chains are slightly distorted from linear and are tilted with respect to the *a*-axis by ±62°. The chains are stacked along [100] with alternating orientation of the chains to produce a herringbone pattern (Figure 10).

(a) **(b)**

Figure 10. Representation of SrNiN showing (**a**) the herringbone stacking, viewed along [010] and (**b**) the zigzagging chains, viewed along [100]. The red, blue, and black spheres represent strontium, nitrogen, and nickel atoms, respectively.

The two strontium positions are four coordinate, surrounded by nitrogen atoms in distorted tetrahedral coordination. Yamamoto et al. proposed that the strontium-centred tetrahedra play an important role in determining the overall structure of the system in $Ca_{1-x}Sr_xNiN$ [69]. As stated previously, as the strontium content increases from *x* = 0 to *x* = 0.5 the *c*-axis expands more than the other two axes. The result is a greater increase in two of the Sr–N distances along *c* compared to the Sr–N distances within *a* or *b*, and hence a greater deviation from the ideal tetrahedron. At *x* = 1, SrNiN adopts an alternate structure with a more favourable structural environment for strontium [69].

Increasing the size of the alkaline earth metal further (i.e., considering the Ba–Ni–N system) also results in a SrNiN-like structure [72]. BaNiN (*Pnma*, *a* = 9.639(3) Å, *b* = 13.674(2) Å, *c* = 5.432(1) Å) shows less distorted $\frac{1}{\infty}[NiN_{2/2}^{2-}]$ chains, with the same repeating zigzag unit altering direction every third nitrogen.

Replacing the transition metal in these linear structures also has an interesting effect on the arrangement of the chain. SrCuN and $Sr(Li_{1-x}Cu_x)N$, $0.33 \leq x \leq 0.53$, are isostructural with SrNiN [21,73], however, the barium-containing compounds show variation in the structure of the chains.

BaCoN (*Pnma*, *a* = 9.599(2) Å, *b* = 23.510(3) Å, *c* = 5.476(2) Å) and BaCuN ($C2_1/c$, *a* = 14.462(2) Å, *b* = 5.5700(8) Å, *c* = 9.478(1) Å, *β* = 102.960(2)°) still show a herringbone stacking of transition metal nitride, $\frac{1}{\infty}[MN_{2/2}^{2-}]$ chains, but these chains differ from SrNiN, showing a more complex alternating pattern, as shown in Figure 11 [66,74].

As Figure 11a shows, the pattern of the chains in BaCoN can be described as altering direction after one nitrogen, followed by a section bent on the second nitrogen, which is followed by a bend on the second nitrogen atom. BaCuN has chains that are bent at every first and second nitrogen atom [66,74].

(a)

(b)
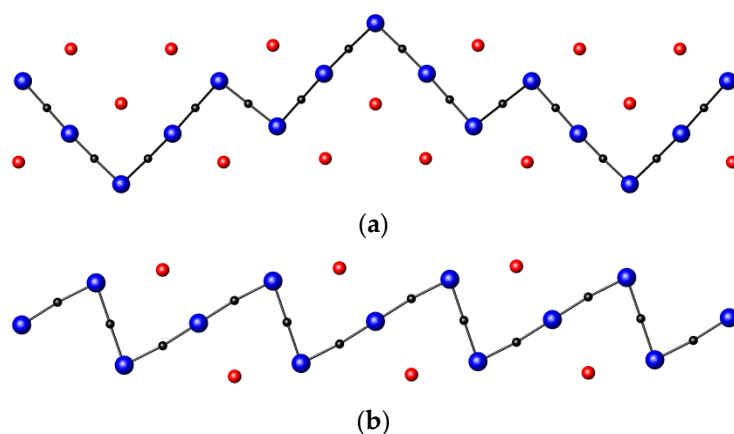
Figure 11. Representations of the chains in (**a**) BaCoN and (**b**) BaCuN. The red, black, and blue spheres represent barium, cobalt/copper, and nitrogen, respectively.

Reducing the transition metal content gives rise to $Ba_8[(NiN)_6]N$ ($C2_1/c$, a = 9.487(4) Å, b = 16.578(6) Å, c = 12.137(7) Å, β = 107.05(5)°) and $Ba_{16}[(CuN)_8][Cu_2N_3][Cu_3N_4]$ ($P2_1/c$, a = 9.5611(4) Å, b = 7.2731(2) Å, c = 13.5225(5) Å, β = 93.115(2)°) [66,75].

$Ba_8[(NiN)_6]N$ contains $\frac{1}{\infty}[NiN_{2/2}^{2-}]$ chains that form distorted, zigzagging helical arrangements. These chains intertwine, as shown in Figure 12a, to give an array of interconnected crosses when viewed along [001]. The barium cation sits in the voids between the chains in both trigonal planar and distorted tetrahedral coordination with nitrogen. The trigonal planar units are corner-connected into layers of six-cornered star arrangements. The tetrahedra show both edge and corner connectivity, forming chains along the *c*-axis.


(a)

(b)
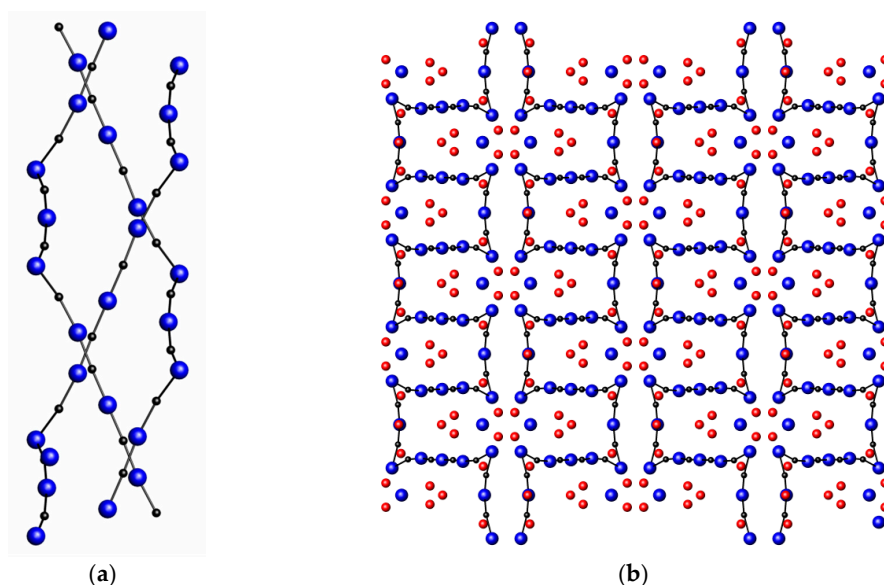
Figure 12. Representation of $Ba_8[(NiN)_6]N$. (**a**) Shows the intertwining $\frac{1}{\infty}[NiN_{2/2}^{2-}]$ chains (for clarity barium has been omitted) and (**b**) shows $Ba_8[(NiN)_6]N$, viewed along [001]. The red, blue, and black spheres represent barium, nitrogen, and nickel, respectively.

$Ba_{16}[(CuN)_8][Cu_2N_3][Cu_3N_4]$ contains isolated $[Cu_2N_3]^{7-}$ and $[Cu_3N_4]^{9-}$ units and $\frac{1}{\infty}[CuN_{2/2}^{2-}]$ chains, which form helical patterns. The $\frac{1}{\infty}[CuN_{2/2}^{2-}]$ chains are bent at every nitrogen, giving the

distinct shape shown in Figure 13. These chains traverse along [010] and are approximately stacked into layers along [001]. The direction of rotation of these helices alternates along these chains.

The layers are then separated by the isolated $[Cu_2N_3]^{7-}$ and $[Cu_3N_4]^{9-}$ units, which are distributed over the same site in a random manner. Both $[Cu_2N_3]^{7-}$ and $[Cu_3N_4]^{9-}$ are near-linear units. $[Cu_2N_3]^{7-}$ is a near-linear chain of five atoms, while $[Cu_3N_4]^{9-}$ forms a zigzag chain which bends at every nitrogen atom. The barium atoms interpenetrate these Cu_xN_y units and separate them.
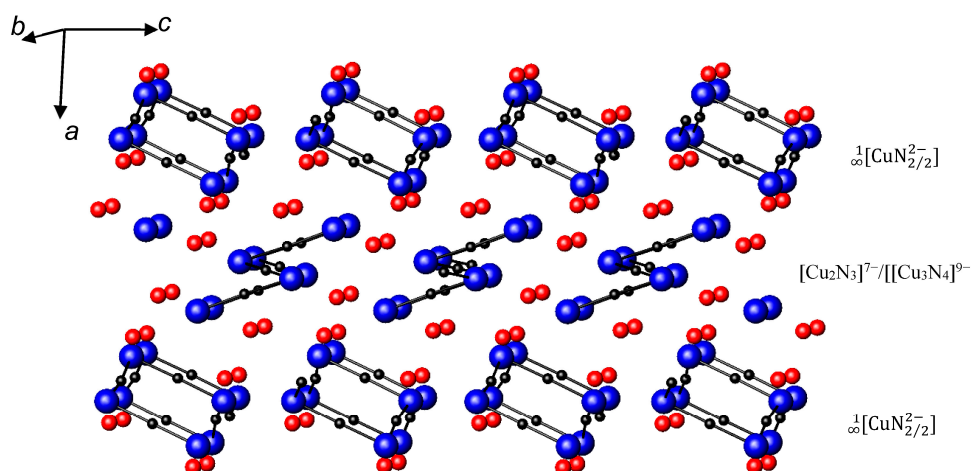
Figure 13. Representation of $Ba_{16}[(CuN)_8][Cu_2N_3][Cu_3N_4]$. The red, blue, and black spheres represent barium, nitrogen, and copper, respectively.

4. Conclusions

Recent developments in the preparation and characterisation of materials have led to the discovery of a large number of new compounds with novel structural features. Despite this, the number of non-oxide materials discovered to date is low in comparison with their oxide counterparts, due to experimental challenges in synthesis and characterisation. The relatively low number of non-oxide compounds acts as an obstacle for understanding these solids, as we cannot categorise these structures to the same extent as we do with oxides and, importantly, the roles of anions other than oxides within crystal structures cannot be investigated in depth. This review aims to outline the structural features of a number of ternary (mixed-metal) nitrides showing quasi-one-dimensional crystal structure. This low-dimensionality of the crystal structure gives rise to high anisotropy in their chemical bonding, which, in turn, is the cause of anisotropy in their physical properties. Selected ternary (mixed-metal) quasi-one-dimensional nitrides have been described and categorised according to the polyhedra forming the one-dimensional chains. The ionic model, often used to describe and discuss crystal structures of oxides, appears to be applicable to a number of nitrides as well, as shown by the linear increase of the unit cell parameters as Ca^{2+} cations are substituted gradually by the larger Sr^{2+} and Ba^{2+} cations in the A_2VN_3 family (A = Ca, Sr, Ba). Where possible, similarities between crystal structures of nitrides with different chemical composition were highlighted and, in some cases, similarities could be highlighted with compounds of a different nature, as in the case of Li_3FeN_2, in which the chains of $^1_\infty[FeN_{4/2}^{3-}]$ tetrahedra are arranged similarly to the chains of $^1_\infty[SiS_{4/2}]$ units found in SiS_2. Finally, this study highlights that the investigation of novel quasi-one-dimensional mixed-metal nitrides would accompany and support the topical research currently carried out on nanowires and nanotubes.

Author Contributions: David Andrew Headspith researched most of the references included in this review and provided drafts of the text, Maria Grazia Francesconi added some references, reviewed the drafts and put together the final manuscript.

Conflicts of Interest: The authors declare no conflict of interest.

References

1. Rao, C.N.R.; Cheetham, A.K.; Mahesh, R. Giant Magnetoresistance and Related Properties of Rare-Earth Manganates and Other Oxide Systems. *Chem. Mater.* **1996**, *8*, 2421–2432. [CrossRef]
2. Rao, C.N.R.; Cheetham, A.K. Giant Magnetoresistance, Charge-Ordering and Related Aspects of Manganates and Other Oxide Systems. *Adv. Mater.* **1997**, *9*, 1009–1017. [CrossRef]
3. Bednorz, J.G.; Müller, K.A. Possible High-Tc Superconductivity in the Ba–La–Cu–O System. *Z. Phys. B Condens. Matter* **1986**, *64*, 189–193. [CrossRef]
4. Wu, M.K.; Ashburn, J.R.; Torng, C.J. Superconductivity at 93 K in a New Mixed-Phase Y–Ba–Cu–O Compound System at Ambient Pressure. *Phys. Rev. Lett.* **1987**, *58*, 908–910. [CrossRef] [PubMed]
5. Titova, S.; Bryntse, I.; Irvine, J.; Mitchell, B.; Balakirev, V. Structural Anomalies of 1223 Hg(Tl)–Ba–Ca–Cu–O Superconductors in the Temperature Range 100–300K. *J. Superconduct.* **1998**, *11*, 471–479. [CrossRef]
6. Smart, L.E.; Moore, E.A. *Solid State Chemistry: An Introduction*, 3rd ed.; CRC Taylor & Francis: London, UK, 2005.
7. Ningthoujam, R.S.; Gajbhive, N.S. Synthesis, electron transport properties of transition metal nitrides and applications. *Prog. Mat. Sci.* **2015**, *70*, 50–154. [CrossRef]
8. Kroschwitz, J.I.; Howe-Grant, M. (Eds.) *Encyclopedia of Chemical Technology*, 4th ed.; John Wiley & Sons: Chichester, UK, 1991–1998.
9. Gregory, D.H. Structural Families in Nitride Chemistry. *J. Chem. Soc. Dalton Trans.* **1999**, *259–270*. [CrossRef]
10. Rouxel, J. (Ed.) *Chrystal Chemistry and Properties of Materials with Quasi-One-Dimensional Structures*; Reidel: Boston, MA, USA, 1986.
11. Lieber, C.M. One-dimensional nanostructures: Chemistry, physics & applications. *Solid State Commun.* **1998**, *107*, 606–616.
12. Jiantao, H.U.; Odom, T.W.; Lieber, C.M. Chemistry and Physics in One Dimension: Synthesis and Properties of Nanowires and Nanotubes. *Acc. Chem. Res.* **1999**, *32*, 435–445.
13. Shi, W.; Hughes, R.W.; Denholme, S.J.; Gregory, D.H. Synthesis design strategies to anisotropic chalcogenide nanostructures. *Cryst. Eng. Commun.* **2010**, *12*, 641–659. [CrossRef]
14. Hahm, J.-I. Zinc Oxide Nanomaterials for Biomedical Fluorescence Detection. *J. Nanosci. Nanotechnol.* **2014**, *14*, 475–486. [CrossRef] [PubMed]
15. Sagawa, T.; Yoshikawa, S.; Imahori, H. One-Dimensional Nanostructured Semiconducting Materials for Organic Photovoltaics. *J. Phys. Chem. Lett.* **2010**, *1*, 1020–1025. [CrossRef]
16. DiSalvo, F.J.; Clarke, S.J. Ternary Nitrides: A Rapidly Growing Class of New Materials. *Curr. Opin. Solid State Mater. Sci.* **1996**, *1*, 241–249. [CrossRef]
17. Zur Loye, H.-C.; Houmes, J.D.; Bem, D.S. Recent developments in ternary nitride chemistry. In *The Chemistry of Transition Metal Carbides and Nitrides*; Oyama, S.T., Ed.; Blackie Academic & Professional: Glasgow, UK, 1996.
18. Brese, N.E.; O'Keeffe, M. Crystal-Chemistry of Inorganic Nitrides. *Struct. Bond.* **1992**, *79*, 307–378.
19. Niewa, R.; Jacobs, H. Group V and VI Alkali Nitridometalates: A Growing Class of Compounds With Structures Related to Silicate Chemistry. *Chem. Rev.* **1996**, *96*, 2053–2062. [CrossRef] [PubMed]
20. Eméleus, H.J.; Sharpe, A.G. (Eds.) *Advances in Inorganic Chemistry and Radiochemistry*, 9th ed.; Academic Press: London, UK, 1966.
21. Gregory, D.H. Nitride Chemistry of the s-block Elements. *Coord. Chem. Rev.* **2001**, *215*, 301–345. [CrossRef]
22. Weast, R.C. (Ed.) *Handbook of Chemistry and Physics*, 51st ed.; The Chemical Rubber Company: Cleveland, OH, USA, 1970.
23. Juza, R.; Langer, K.; von Benda, K. Ternary Nitrides, Phosphides, and Arsenides of Lithium. *Angew. Chem. Int. Ed. Engl.* **1968**, *7*, 360–370. [CrossRef]
24. Addison, C.C.; Pulham, R.J.; Trevillion, E.A. Reaction between Barium and Nitrogen in Liquid Sodium—Solubility Studies. *J. Chem. Soc. Dalton Trans.* **1975**, 2082–2085. [CrossRef]
25. Brese, N.E.; O'Keeffe, M. Synthesis, Crystal-Structure and Physical-Properties of Sr_2N. *J. Solid State Chem.* **1990**, *87*, 134–140. [CrossRef]

26. Vajenine, G.V.; Grzechnik, A.; Syassen, K.; Loa, I.; Hanfland, M.; Simon, A. Interplay of Metallic and Ionic Bonding in Layered Subnitrides AE$_2$N (AE = Ca, Sr or Ba) under High Pressure. *C. R. Chim.* **2005**, *8*, 1897–1905. [CrossRef]

27. Beilby, G.T.; Henderson, G.G. The Action of Ammonia on Metals at High Temperature. *J. Chem. Soc. Trans.* **1901**, 1245–1265. [CrossRef]

28. Gomathi, A. Ternary Metal Nitrides by the Urea Route. *Mater. Res. Bull.* **2007**, *42*, 870–874. [CrossRef]

29. Zhao, H.; Lei, M.; Chen, X.; Tang, W. Facile Route to Metal Nitrides through Melamine and Metal Oxides. *J. Mater. Chem.* **2006**, *16*, 4407–4412. [CrossRef]

30. Weil, K.S.; Kumta, P.N. Synthesis of Ternary Transition Metal Nitrides Using Chemically Complexed Precursors. *Mater. Sci. Eng. B* **1996**, *38*, 109–117. [CrossRef]

31. Herle, P.S.; Hegde, M.S.; Sooryanarayana, K.; Row, T.N.G.; Subbanna, G.N. Ni$_2$Mo$_3$N: A New Ternary Interstitial Nitride with a Filled Beta-Manganese Structure. *Inorg. Chem.* **1998**, *37*, 4128–4130. [CrossRef]

32. Bem, D.S.; Gibson, C.P.; zur Loye, H.-C. Synthesis of Intermetallic Nitrides by Solid-State Pecursor Reduction. *Chem. Mater.* **1993**, *5*, 397–399. [CrossRef]

33. Prior, T.J.; Battle, P.D. Facile Synthesis of Interstitial Metal Nitrides with the Filled Beta-Manganese Structure. *J. Solid State Chem.* **2003**, *172*, 138–147. [CrossRef]

34. Prior, T.J.; Oldham, S.E.; Couper, V.J.; Battle, P.D. Ferromagnetic Nitrides with the Filled Beta-Mn Structure Fe$_{2-x}$M$_x$Mo$_3$N (M = Ni, Pd, Pt). *Chem. Mater.* **2005**, *17*, 1867–1873. [CrossRef]

35. Prior, T.J.; Battle, P.D. Superparamagnetism and Metal-Site Ordering in Quaternary Nitrides with the η-Carbide Structure. *J. Mater. Chem.* **2004**, *14*, 3001–3007. [CrossRef]

36. Houmes, J.D.; zur Loye, H.-C. Plasma Nitridation of Metal Oxides. *Chem. Mater.* **1996**, *8*, 2551–2553. [CrossRef]

37. Kroke, E. High-Pressure Synthesis of Novel Binary Nitrogen Compounds of Main Group Elements. *Angew. Chem. Int. Ed. Engl.* **2002**, *41*, 77–82. [CrossRef]

38. Niewa, R.; DiSalvo, F.J. Recent Developments in Nitride Chemistry. *Chem. Mater.* **1998**, *10*, 2733–2752. [CrossRef]

39. Rauch, P.E.; Simon, A. The New Subnitride NaBa$_3$N—An Extension of Alkali-Metal Suboxide Chemistry. *Angew. Chem. Int. Ed. Engl.* **1992**, *31*, 1519–1521. [CrossRef]

40. Snyder, G.J.; Simon, A. The Infinite Chain Nitride Na$_5$Ba$_3$N—A One-Dimensional Void Metal. *J. Am. Chem. Soc.* **1995**, *117*, 1996–1999. [CrossRef] [PubMed]

41. Simon, A. Group 1 and 2 Suboxides and Subnitrides—Metals with Atomic Size Holes and Tunnels. *Coord. Chem. Rev.* **1997**, *163*, 253–270. [CrossRef]

42. Gudat, A.; Kniep, R.; Rabenau, A.; Bronger, W.; Ruschewitz, U. Li$_3$FeN$_2$, a Ternary Nitride with $^1_\infty[\text{FeN}^{3-}_{4/2}]$ Chains—Crystal Structure and Magnetic Properties. *J. Less Common Met.* **1990**, *161*, 31–36. [CrossRef]

43. Cordier, G.; Gudat, A.; Kniep, R.; Rabenau, A. LiCaN and Li$_4$SrN$_2$ Derivatives of the Fluorite and Lithium Nitride Structures. *Angew. Chem. Int. Ed. Engl.* **1989**, *28*, 1702–1703. [CrossRef]

44. Shannon, R.D.; Prewitt, C.T. Effective Ionic Radii in Oxides and Fluorides. *Acta Crystallogr. B* **1969**, *25*, 925–946. [CrossRef]

45. Baur, W.H. Effective Ionic Radii in Nitrides. *Cryst. Rev.* **1987**, *1*, 59–83. [CrossRef]

46. Peters, J.; Krebs, B. Silicon Disulfide and Silicon Diselenide—A Reinvestigation. *Acta Crystallogr. B* **1982**, *38*, 1270–1272. [CrossRef]

47. Makovicky, E. Crystal Structures of Sulfides and Other Chalcogenides. *Rev. Miner. Geochem.* **2006**, *61*, 7–125. [CrossRef]

48. Yamane, H.; DiSalvo, F.J. Ba$_3$Ga$_2$N$_4$. *Acta Crystallogr. C* **1996**, *52*, 760–761. [CrossRef]

49. Blasé, W.; Cordier, G.; Ludwig, M.; Kniep, R. Sr$_3$[Al$_2$N$_4$]: A Nitridoaluminate with Corrugated Tetrahedral Chains $^1_\infty[\text{AlN}^{3-}_{4/2}]$. *Z. Naturforsch. B* **1994**, *49*, 501.

50. Clarke, S.J.; DiSalvo, F.J. Synthesis and Structure of One-, Two- and Three-Dimensional Alkaline Earth Metal Gallium Nitrides: Sr$_3$Ga$_2$N$_4$, Ca$_3$Ga$_2$N$_4$ and Sr$_3$Ga$_3$N$_5$. *Inorg. Chem.* **1997**, *36*, 1143–1148. [CrossRef] [PubMed]

51. Ludwig, M.; Niewa, R.; Kniep, R. Dimers [Al$_2$N$_6$]$^{12-}$ and Chains $^1_\infty[\text{AlN}^{3-}_{\frac{4}{2}}]$ in the Crystal Structures of Ca$_6$[Al$_2$N$_6$] and Ba$_3$[Al$_2$N$_4$]. *Z. Naturforsch. B* **1999**, *54*, 461–465. [CrossRef]

52. Niewa, R.; Zherebtsov, D.A.; Borrmann, H.; Kniep, R. Preparation and Crystal Structure of Li$_4$TaN$_3$. *Z. Anorg. Allg. Chem.* **2002**, *628*, 2505–2508. [CrossRef]

53. Jacobs, H.; Niewa, R. Synthesis and Crystal Structure of a Sodium Nitrido Tungstate (VI), Na_3WN_3. *Eur. J. Solid State Inorg. Chem.* **1994**, *31*, 105–113.

54. Rauch, P.E.; DiSalvo, F.J.; Brese, N.E.; Partin, D.E.; O'Keeffe, M. Synthesis and Neutron Diffraction Study of Na_3WN_3 and Na_3MoN_3. *J. Solid State Chem.* **1994**, *110*, 162–166. [CrossRef]

55. Niewa, R.; Jacobs, H. $Na_5Rb(WN_3)_2$ and $Na_5Cs(WN_3)_2$, Two New Sodium Nitrido Tungstates(VI) with the Heavier Alkali Metals Rubidium and Cesium. *J. Alloys Comp.* **1996**, *234*, 171–177. [CrossRef]

56. Niewa, R.; Jacobs, H. Na_2KWN_3 and $Na_{11}Rb(WN_3)_4$, Two New Alkali Metal Nitrido Tungstates(VI) with Closely Related Structures. *J. Alloys Comp.* **1996**, *233*, 61–68. [CrossRef]

57. Bowman, A.; Gregory, D.H. Synthesis and Characterisation of the Ternary Nitride Sr_2TaN_3. *J. Alloys Comp.* **2003**, *348*, 80–87. [CrossRef]

58. Zherebtsov, D.A.; Aksel'rud, L.G.; Niewa, R. Crystal Structure of Dicalcium Trinitrido Monovanadate(V), Ca_2VN_3. *Z. Kristallogr. New Cryst. Struct.* **2002**, *217*, 469.

59. Seeger, O.; Hofmann, M.; Strähle, J.; Laval, J.P.; Frit, B. Synthesis and Structure of $BaZrN_2$ and Ba_2NbN_3. *Z. Anorg. Allg. Chem.* **1994**, *620*, 2008–2013. [CrossRef]

60. Benz, R.; Zachariasen, W.H. Crystal Structures of Th_2CrN_3, Th_2MnN_3, U_2CrN_3 and U_2MnN_3. *J. Nucl. Mater.* **1970**, *37*, 109–113. [CrossRef]

61. Broll, S.; Jeitschko, W. The Ternary Rare-Earth Chromium Nitrides Ce_2CrN_3 and $Ln_3Cr_{10-x}N_{11}$ with Ln = La, Ce, Pr. *Z. Naturforsch. B* **1995**, *50*, 905–912. [CrossRef]

62. Niewa, R.; Vajenine, G.V.; DiSalvo, F.J.; Luo, H.; Yelon, W.B. Unusual Bonding in Ternary Nitrides: Preparation, Structure and Properties of Ce_2MnN_3. *Z. Naturforsch. B* **1998**, *53*, 63–74. [CrossRef]

63. Landrum, G.A.; Dronskowski, R.; Niewa, R.; DiSalvo, F.J. Electronic Structure and Bonding in Cerium Nitride Compounds: Trivalent Versus Tetravalent Cerium. *Chem. Eur. J.* **1999**, *5*, 515–522. [CrossRef]

64. Niewa, R.; Hu, Z.; Grazioli, C.; Rößler, U.; Golden, M.S.; Knupfer, M.; Fink, J.; Giefers, H.; Wortmann, G.; de Groot, F.M.F.; et al. XAS Spectra of $Ce_2[MnN_3]$ at the $Ce–M_{4,5}$, $Ce–L_3$, $Mn–L_{2,3}$ and N–K threshholds. *J. Alloys Comp.* **2002**, *346*, 129–133. [CrossRef]

65. Höhn, P.; Haag, S.; Milius, W.; Kniep, R. $Sr_2LiFe_2N_3$ and $Ba_2LiFe_2N_3$—Nitridoferrate(II) Isotypes with $^1_\infty[(FeN_{3/2})^{5-}_2]$ Anions. *Angew. Chem. Int. Ed. Engl.* **1991**, *30*, 831–832. [CrossRef]

66. Niewa, R.; DiSalvo, F.J. Breaking up Chains: The Nitridocuprates(I) BaCuN $Ba_{16}[(CuN)_8][Cu_2N_3][Cu_3N_4]$ and $Ca_4Ba[CuN_2]_2$. *J. Alloys Comp.* **1998**, *279*, 153–160. [CrossRef]

67. Gudat, A.; Kniep, R.; Maier, J. $Ca[(Ni_{1-x}Li_x)N]$: Limited solid solutions ($0 \leq x \leq 0.58$) in the system Ca[NiN] (Y[CoC]-type structure)-Ca[LiN] (modified fluorite-type structure). *J. Alloys Comp.* **1992**, *186*, 339–345. [CrossRef]

68. Chern, M.Y.; DiSalvo, F.J. Synthesis, Structure, Electric and Magnetic Properties of CaNiN. *J. Solid State Chem.* **1990**, *88*, 459–464. [CrossRef]

69. Yamamoto, T.; Kikkawa, S.; Kanamaru, F. Preparation of New Ternary Nitrides CaMN (M = Co, Ni). *Solid State Ionics* **1993**, *63–65*, 148–153. [CrossRef]

70. Yamamoto, T.; Kikkawa, S.; Kanamaru, F. Preparation, Crystal Structure and Properties of a New Double Metal Nitride SrNiN and of $Ca_{1-x}Sr_xNiN$ ($0 \leq x \leq 0.5$). *J. Solid State Chem.* **1995**, *115*, 353–359. [CrossRef]

71. Cordier, G.; Gudat, A.; Kniep, R.; Rabenau, A. LiSrN—A 3-Dimensional Structural Arrangement of Corner and Edge Sharing Orthorhombic Bipyramids $Ni_{2/2}Sr_{4/4}$. *Angew. Chem. Int. Ed. Engl.* **1989**, *28*, 201–202. [CrossRef]

72. Gudat, A.; Haag, S.; Kniep, R.; Rabenau, A. On the Crystal Structure of BaNiN a Low Valency Nitridoniccolate(I). *J. Less Common Met.* **1990**, *159*, L29–L31. [CrossRef]

73. DiSalvo, F.J.; Trail, S.S.; Yamane, H.; Brese, N.E. The Crystal Structure of $Sr_6Cu_3N_5$ with Isolated, Bent $(Cu_2N_3)^{7-}$ anions and the Single Crystal Structure Determination of SrCuN. *J. Alloys Comp.* **1997**, *255*, 122–129. [CrossRef]

74. Tennstedt, A.; Kniep, R. BaCoN—A Low Valency Nitridocobaltate with Angled Chains $^1_\infty[CoN^{2-}_{2/2}]$. *Z. Anorg. Allg. Chem.* **1994**, *620*, 1781–1785. [CrossRef]

75. Gudat, A.; Milius, W.; Haag, S.; Kniep, R.; Rabenau, A. On the Crystal-Structure of $Ba_8Ni_6N_7$, A Low Valency Nitridoniccolate with Infinite Helical [Ni–N] Zigzag Chains. *J. Less Common Met.* **1991**, *168*, 305–312. [CrossRef]